Journal of Agrometeorology

(A publication of Association of Agrometeorologists)

ISSN : 0972-1665 (print), 2583-2980 (online)
Vol. No. 28 (1) : 44 - 51 (March - 2026)
https://doi.org/10.54386/jam.v28i1.3113
https://journal.agrimetassociation.org/index.php/jam

Research paper

Spatiotemporal analysis of Drought characteristics in Nineveh, Iraq using the Standardized Precipitation Evapotranspiration Index (SPEI)

KHALID QARAGHULI[1,2], M. F. MURSHED[1*] and M. AZLIN M. SAID[1]

[1]*School of Civil Engineering, Engineering Campus, Universiti Sains Malaysia, Malaysia.*
[2]*Al-Mussaib Technical Institute, Al-Furat Al-Awsat Technical University, Babil, Iraq.*
[*]*Corresponding Author email: cefaredmurshed@usm.my*

ABSTRACT

Combining station observations with bias-corrected gridded climate data is crucial for reliable drought assessment in data-sparse regions. This study investigates the spatiotemporal characteristics of drought in Nineveh, Iraq, using the Standardized Precipitation Evapotranspiration Index at three- and six-month timescales (SPEI03 and SPEI06). Monthly station observations (1992-2013) were used to bias-correct TerraClimate data (2001-2023), which were then utilized to extend the record and compute SPEIs based on precipitation and potential evapotranspiration (PET). Drought frequency, duration, severity, and intensity were quantified, and trends were assessed using the Mann–Kendall test and Sen's slope estimator. Results show notable interannual variability and a clear shift toward more frequent, severe, and persistent droughts in recent decades. The northern and northeastern areas emerged as drought hotspots, with Tel-Afar station experiencing the longest and most severe events. Comparisons between 2001–2011 and 2012–2023 reveal a marked intensification and expansion of severe and extreme drought zones. Trend analysis confirms widespread declines in moisture availability, especially for SPEI06, indicating increased exposure to prolonged water deficits. These findings highlight substantial spatial heterogeneity and emphasize the need for localized drought adaptation, improved water resource management, and early-warning systems to mitigate escalating risks to agriculture and livelihoods under a changing climate.

***Keywords*:** Drought, Spatiotemporal analysis, SPEI, Climate change, Gridded data

Climate change increases the frequency, persistence, and severity of droughts by altering precipitation and boosting evapotranspiration. Global droughts have risen by nearly 29% since 2000, with further increases expected under high-emission scenarios (Rahman *et al.,* 2025). Unlike sudden hazards, droughts develop gradually yet cause severe socio-economic and environmental impacts. Prolonged dry spells and rising temperatures disrupt agriculture, water resources, forestry, and public health, threatening food security and livelihoods. Extended droughts also accelerate land degradation and wildfire risks, compounding these vulnerabilities (Terzi & Önöz, 2025).

The Food and Agriculture Organization (FAO) and the UN World Food Programme (WFP) highlight Iraq's exposure to heat waves, dust storms, and prolonged droughts. Iraq ranks among the world's five most climate-vulnerable countries and continues to face worsening food insecurity and declining water supplies (Hashim *et al.,* 2025). Accurate drought monitoring in Iraq is challenging due to sparse station networks and frequent data gaps from equipment failures, closures, or logistical issues. These limitations hinder reliable trend analysis, early warning, and adaptive management (Sa'adi *et al.,* 2023). To address this, gridded climate datasets offer long-term, spatially continuous records that bridge gaps in conventional monitoring (Newman *et al.,* 2024).

A clear understanding of drought dynamics requires systematic analysis of its spatiotemporal characteristics, including severity, duration, and extent. Effective drought assessment depends on indices that translate climate data into actionable information for early warning and management. Various drought indices have been developed for different monitoring needs (Prasad *et al.,* 2025). Examples include the Palmer Drought Severity Index (PDSI), which accounts for soil moisture, and the Standardized Precipitation Index (SPI), which evaluates precipitation anomalies at multiple

***Article info - DOI*:** *https://doi.org/10.54386/jam.v28i1.3113*
Received:06 July 2025; Accepted: 13 November 2025; Published online : 1 March 2026

Table 1: Description of meteorological stations

Station	Name	Latitude	Longitude	Altitude (m)
1	Al-Baaj	36° 02’	41° 48’	321
2	Makhmour	35° 46’	43° 35’	270
3	Mosul	36° 19’	43° 09’	223
4	Rabiah	36° 48’	42° 06’	382
5	Sinjar	36° 19’	41° 50’	465
6	Tel-Abta	35° 55’	42° 24’	200
7	Tel-Afar	36° 22’	42° 06’	273

timescales. However, indices based only on precipitation or soil moisture often fail to capture the impact of rising temperatures and increased evaporative demand. To address this, the Standardized Precipitation Evapotranspiration Index (SPEI; Vicente-Serrano *et al*., 2010) integrates both precipitation and potential evapotranspiration, combining the PDSI’s sensitivity to evaporation with the SPI’s temporal flexibility. The SPEI has proven effective in diverse climates, including China, Hungary, southern Africa, and India (Mokhtar *et al.,* 2022).

Therefore, this study aims to assess the spatiotemporal characteristics of drought in Nineveh, Iraq, including severity, duration, spatial distribution, and trend, by applying the SPEI at short- (SPEI-03) and medium-term (SPEI-06) timescales, using a combination of station observations and bias-corrected high-resolution TerraClimate data. The novelty of this work lies in extending limited station records with bias-corrected gridded data to produce a long-term drought assessment. The study contributes to improving drought monitoring and understanding in data-scarce regions of Iraq.

MATERIAL AND METHODS

Study area

This research specifically examines the Nineveh governorate (Fig. 1), often referred to as Iraq’s “breadbasket” due to its extensive rainfed cereal production, mainly wheat and barley. Located in northwestern Iraq, Nineveh spans approximately 32,308 km² between 41° 25′ and 44° 15′ E longitude and 34° 15′ to 37° 30′ N latitude (Qaraghuli *et al.,* 2024). The governorate’s topography is predominantly flat, except for mountainous and uplifted terrains in the northeast, where elevations exceed 1,000 meters, contrasting with lowland areas in the south at approximately 100 meters. Climatically, Nineveh experiences a semi-arid climate with pronounced seasonal variations, influenced by diverse terrain and regional circulation patterns. According to the Köppen-Geiger classification, Mosul lies at the intersection of the Mediterranean (Csa) and Subtropical Steppe (Bsh) climatic zones. The Mediterranean climate (Csa) is characterized by cold, wet winters and hot, dry summers, while the Subtropical Steppe climate (Bsh) exhibits moderately cold winters and extremely hot, arid summers. Winters in Nineveh are mild but not tropical, with an average January temperature of 7°C. Summers, in contrast, are extremely hot and arid, with peak daytime temperatures reaching 43°C in July and August, though air humidity remains low. Annual precipitation averages 365 mm, predominantly occurring between November and April.

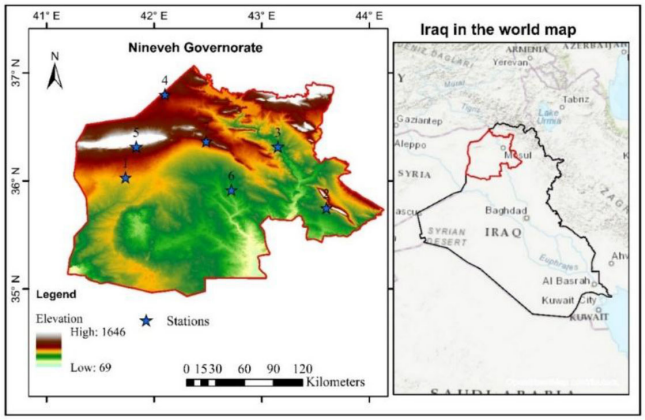

Fig. 1: Study area and the location of the meteorological stations

Station data

To support this research, monthly meteorological observations were collected from seven stations across the Nineveh governorate, Iraq, for the period 1992–2013. The dataset includes key climatic variables such as precipitation (P), maximum temperature (Tmax), minimum temperature (Tmin), mean temperature (Tmean), relative humidity (RH), wind speed (WS), and sunshine duration (SS). These records were obtained from the Iraqi Meteorological Organization and Seismology (IMOS), the primary authority responsible for climate and weather monitoring in Iraq. The description of the meteorological stations is detailed in Table 1.

Gridded data

TerraClimate is a high-resolution global dataset that offers monthly climate and water balance variables for terrestrial surfaces worldwide from 1958 to the present. With a spatial resolution of approximately 4 km (1/24°) and monthly temporal coverage (Al-Yaari *et al.,* 2024) timing, and spatial variability of these changes. While considerable attention has been paid to current and future changes in temperature patterns, comparatively less attention has been devoted to water availability for humans and ecosystems. The aridity index (AI. The gridded datasets were bias-corrected using the Empirical Quantile Mapping (EQM) method to align with observed station data.

Integration of station and gridded data

To ensure temporal continuity and spatial completeness, ground-based station records (1992–2013) were integrated with TerraClimate gridded data (2001–2023). The station data were primarily used to correct gridded data and to analyze station-based drought. The overlapping period (2001–2013) was employed to bias-correct TerraClimate precipitation and PET using the Empirical Quantile Mapping (EQM) technique. This correction aligned the statistical distribution of the gridded data with the observed station measurements, minimizing systematic deviations. Following the bias correction, the adjusted TerraClimate dataset (2001–2023) was utilized both to extend the time series beyond 2013 and to enable spatially continuous calculation of the SPEI-03 and SPEI-06 across the entire study area.

Table 2: Definitions and calculation formulas for drought characteristic metrics

Metric	Description	Formula
Number of drought months (NDM)	Total months with SPEI < 0, indicating the frequency of drought conditions.	/
Longest drought duration (LDD)	Longest consecutive sequence of months with SPEI < 0.	/
Number of drought events (NDE)	Total count of distinct drought events (consecutive months with SPEI < 0).	/
Average drought duration (AvgDur)	Average duration of drought events.	$AvgDur = \frac{\sum_{i=1}^{n} d_i}{n}$
Drought deverity (S)	Sum of absolute negative SPEI values during a drought event.	$S_j = \left\lvert \sum_{i=1}^{D_j} SPEI_{i,j} \right\rvert$
Average severity (AvgSev)	Cumulative severity is divided by total drought events.	$AvgSev = \frac{S}{n}$
Maximum severity (MaxSev)	Largest cumulative SPEI deficit in the study period.	/
Drought intensity (DI)	Severity divided by duration; average and maximum intensities calculated.	$DI = \frac{Severity}{Duration}$
Drought area (DA)	Spatial extent of drought conditions as % of total area.	$DA = \frac{\sum_{i=1}^{n} d_a}{n_a} \times 10$

Table 3: Percentage distribution of SPEI03 and SPEI06 categories across stations from 1992-2023

Station	Extreme wet	Severe Wet	Moderate wet	Mild Wet	Mild drought	Moderate drought	Severe drought	Extreme drought
				SPEI03				
Al-Baaj	1.56	7.03	9.11	32.29	32.03	11.72	3.13	3.13
Makhmour	3.13	2.86	10.94	33.59	33.85	8.85	4.17	2.60
Mosul	1.82	3.91	9.90	35.68	28.13	13.80	4.43	2.34
Rabiah	1.56	4.43	10.42	34.64	29.95	11.72	4.69	2.60
Sinjar	3.13	4.17	7.55	38.54	27.86	10.94	5.99	1.82
Tel-Abta	1.04	4.95	8.59	36.72	27.34	12.24	7.81	1.30
Tel-Afar	1.82	2.60	14.58	29.17	33.33	10.42	4.95	3.13
				SPEI06				
Al-Baaj	1.04	5.99	10.68	31.25	33.33	12.50	2.34	2.86
Makhmour	3.13	3.65	9.64	32.81	35.94	8.07	3.65	3.13
Mosul	1.56	4.95	10.16	36.46	27.08	12.24	5.47	2.08
Rabiah	1.04	4.43	11.20	32.81	31.51	10.94	6.25	1.82
Sinjar	3.13	2.86	9.64	38.28	28.65	8.07	7.55	1.82
Tel-Abta	2.60	3.91	7.03	39.32	29.17	9.11	7.29	1.56
Tel-Afar	1.82	3.39	11.98	31.77	34.38	8.33	7.03	1.30

Standardized precipitation evapotranspiration index (SPEI)

Using the SPEI package in R, SPEI values were calculated at two timescales: three months (SPEI03) to capture short-term variability and six months (SPEI06) to reflect medium-term drought dynamics. The SPEI was computed at two stages: (i) station-based SPEI using observed and gridded data for the period 1992–2023, and (ii) spatially distributed SPEI across the entire study area using bias-corrected TerraClimate data for 2001–2023. This dual approach allowed for both point-based and regional-scale assessment of drought variability. Drought conditions were categorized into severity levels based on SPEI values (Extreme wet (≥ 2.00), Severe wet (1.50 to 1.99), Moderate wet (1.00 to1.49), Mild wet (0.00 to 0.99), Mild drought (0.00 to -0.99), Moderate drought (-1.00 to -1.49), Severe drought (-1.50 to -1.99), Extreme drought (≤ -2.00), enabling a systematic assessment of drought characteristics across the region.

Drought characteristic metrics

Drought events were identified based on a threshold where SPEI values fell below zero (SPEI < 0), indicating dry conditions. After identifying these events, their characteristics were assessed using metrics detailed in Table 2. Each drought characteristic was selected to represent a specific aspect of drought behavior: the number of drought months (NDM) and number of drought events

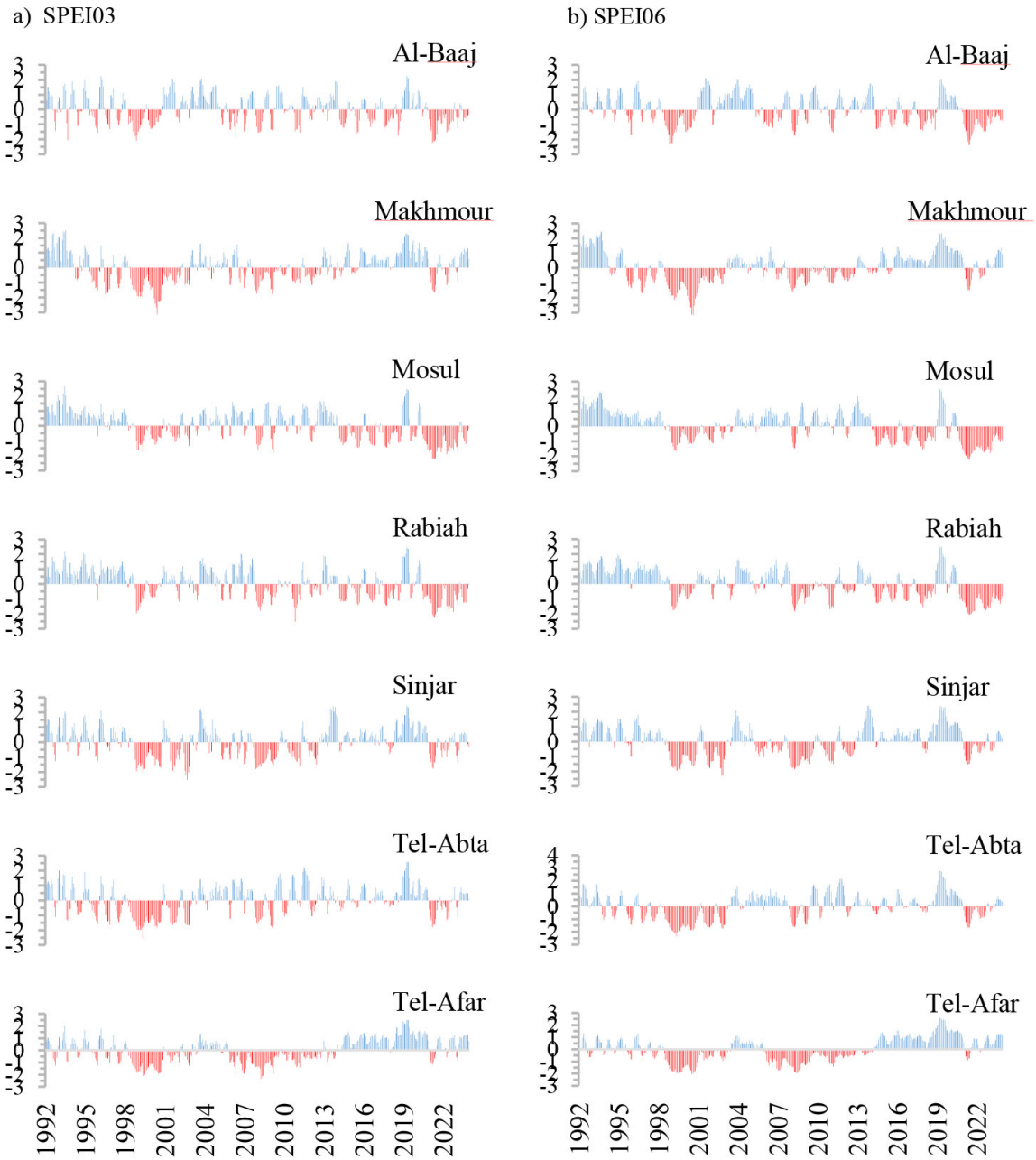

Fig. 2: Temporal evolution of SPEI03 and SPEI06 from 1992-2023 for the seven stations

(NDE) describe frequency; the longest and average durations (LDD, AvgDur) indicate temporal persistence; maximum and average severity (MaxSev, AvgSev) reflect cumulative moisture deficit; and average and maximum intensity (AvgInt, MaxInt) describe drought strength relative to duration. The drought area (DA) expresses the spatial extent of drought conditions. Together, these metrics provide a comprehensive understanding of drought magnitude, persistence, and spatial coverage across stations and timescales.

RESULTS AND DISCUSSION

Temporal drought variability

Fig. 2 shows the SPEI03 and SPEI06 time series from 1992 to 2023 for each station, highlighting short- and medium-term drought dynamics. SPEI03 shows greater temporal variability than SPEI06, capturing more frequent but shorter droughts, while SPEI06 reflects longer, sustained dry periods. Frequency distributions in Fig. 3 further illustrate spatial heterogeneity, with some stations showing more frequent shifts between wet and dry phases due to local climate variability. Focusing on SPEI06 and excluding mild droughts (0 > SPEI06 > -1), the years 1998, 1999, 2000, 2008, and 2021 emerge as notable drought years, marked by severe, sustained dryness across multiple stations. These drought years correspond to documented regional dry anomalies linked to strong El Niño episodes and persistent reductions in winter precipitation across Iraq. However, clear spatial differences persist; some stations show

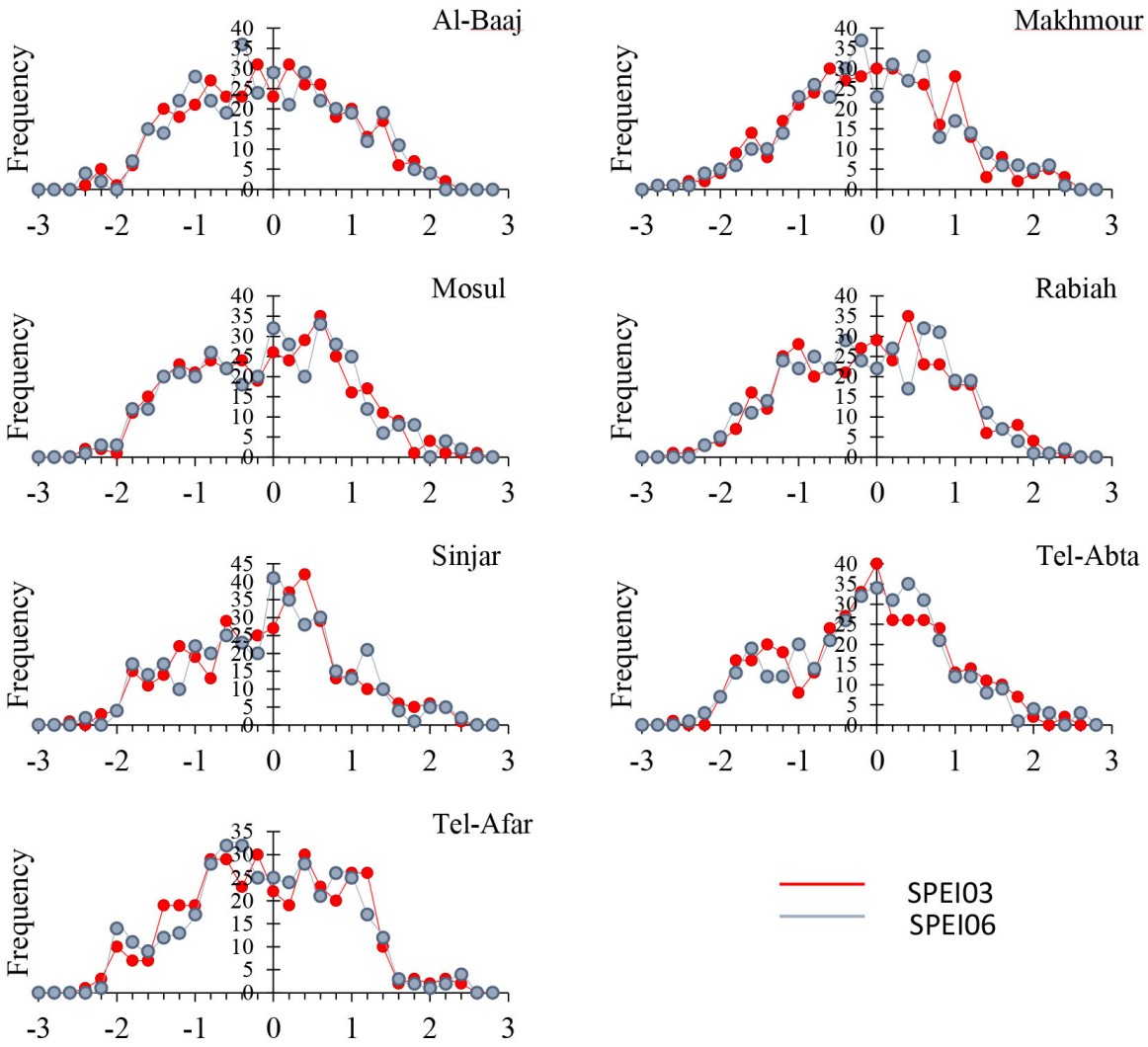

Fig. 3: Frequency distribution of SPEI03 and SPEI06 values in 0.2 intervals from 1992 to 2023

weaker drought signals during these periods, reflecting the influence of local factors such as topography, elevation, and hydrological setting on drought severity and duration. These variations indicate that drought occurrence in Nineveh is not uniform but modulated by mesoscale climatic and physiographic controls. Stations located at higher elevations (e.g., Rabiah and Sinjar) exhibit relatively moderate drought intensity, likely due to orographic enhancement of rainfall, whereas low-lying areas such as Mosul and Tel-Abta stations show more persistent negative SPEI values, suggesting higher exposure to prolonged aridity.

Classification of drought occurrences using SPEI03 and SPEI06 (Table 3) reveals clear spatial differences in drought frequency and severity across the seven meteorological stations. Mild drought was the most common category, especially at Makhmour station, which recorded the highest frequency of both short- and medium-term dry spells. Moderate drought was more frequent at Al-Baaj and Mosul stations, indicating recurrent drought episodes. Severe drought conditions occurred most often at stations Sinjar, Tel-Abta, and Tel-Afar, with Tel-Abta station showing the highest occurrence in SPEI03 and Sinjar in SPEI06, reflecting greater susceptibility to prolonged dry periods. Extreme drought was rare but most frequent at stations Al-Baaj, Makhmour, and Tel-Afar. These results underscore the spatial variability of drought conditions across the study area and highlight that Sinjar, Tel-Abta, and Tel-Afar stations are especially prone to severe, long-lasting droughts, pointing to the need for localized mitigation strategies to address station-specific vulnerabilities.

Drought characteristic metrics across stations

Table 4 presents the drought characteristics derived from SPEI03 and SPEI06 across the seven meteorological stations, revealing pronounced spatial variability in drought frequency, duration, severity, and intensity. Under SPEI03, the number of drought events (NDE) ranged from 24 at Tel-Afar to 36 at Sinjar, indicating that Sinjar faced more frequent, short-lived droughts, while Tel-Afar experienced fewer but more prolonged events. This is supported by Tel-Afar's highest average drought duration (8.17 months) compared to Sinjar's shortest (4.97 months), highlighting

Table 4: Drought metrics for the studied stations based on SPEI03 and SPEI06

	Station	NDM	LDD	MaxSev	AvgSev	NDE	AvgDur	AvgInt	MaxInt
SPEI03	Al-Baaj	191	24	25.79	4.50	34	5.62	0.80	1.07
	Makhmour	189	46	58.15	5.22	29	6.52	0.80	1.26
	Mosul	184	34	48.21	5.46	29	6.34	0.86	1.42
	Rabiah	187	34	41.55	4.70	33	5.67	0.83	1.22
	Sinjar	179	27	32.92	4.20	36	4.97	0.84	1.22
	Tel-Abta	183	32	44.62	4.58	33	5.55	0.83	1.39
	Tel-Afar	196	67	62.22	6.55	24	8.17	0.80	0.93
SPEI06	Al-Baaj	192	37	37.68	6.12	25	7.68	0.80	1.02
	Makhmour	193	57	69.26	6.77	22	8.77	0.77	1.22
	Mosul	178	41	56.43	7.41	21	8.48	0.87	1.38
	Rabiah	191	40	52.88	8.65	18	10.61	0.82	1.32
	Sinjar	174	27	36.41	6.79	22	7.91	0.86	1.35
	Tel-Abta	180	35	50.67	5.53	27	6.67	0.83	1.45
	Tel-Afar	193	85	74.36	10.97	14	13.79	0.80	0.87

rapid but recurrent dry spells at Sinjar. Drought severity patterns reflected these trends, with Tel-Afar recording the highest average severity (AvgSev = 6.55) and maximum severity (MaxSev = 62.22), pointing to particularly intense drought events. In contrast, other stations showed lower average severities, ranging from 4.20 at Sinjar to 5.46 at Mosul. Average drought intensity (AvgInt) was fairly consistent across stations (0.80–0.86), but maximum intensity (MaxInt) varied more widely, with Mosul peaking at 1.42, suggesting short but intense droughts.

SPEI06 metrics reflected longer-term moisture deficits, with fewer but more persistent and severe droughts. Tel-Afar again stood out, with the fewest events (14) but the longest average duration (13.79 months) and highest average severity (AvgSev = 10.97), confirming its vulnerability to prolonged drought. Other stations showed lower average severities, from 5.53 (Tel-Abta) to 8.65 (Rabiah). Intensity under SPEI06 showed more variation than SPEI03, with AvgInt ranging from 0.77 to 0.87 and MaxInt reaching 1.45 at Tel-Abta, indicating local exposure to extreme drought intensity. Overall, these results reveal significant spatial differences in drought characteristics. Tel-Afar consistently emerged as the most drought-prone, marked by persistent and severe droughts, especially under SPEI06, while stations Sinjar and Mosul faced shorter, more frequent events. This variability underscores the need for localized drought management and early warning systems tailored to station-specific risks, particularly for areas like Tel-Afar where sustained moisture deficits could have serious ecological and socio-economic impacts.

These spatial contrasts are mainly influenced by topography and temperature gradients, where low-lying western stations experience higher evapotranspiration and longer droughts, while elevated sites receive more intermittent rainfall. The stronger persistence in SPEI06 further reflects cumulative moisture deficits driven by sustained warming and reduced precipitation. Overall, Tel-Afar remains the most drought-prone, emphasizing the need for localized drought monitoring and adaptive water management in these vulnerable areas.

Spatial analysis of drought

The spatial distribution of key drought metrics, number of drought months (NDM), maximum severity (MaxSev), and maximum intensity (MaxInt), was assessed using SPEI03 and SPEI06 for two periods: 2001–2011 and 2012–2023. These metrics provide insights into how drought conditions have evolved across the study area. Fig. 4 illustrates these spatial patterns, showing a clear shift toward more intense and persistent droughts in the later period. From 2001–2011, drought conditions were relatively moderate. SPEI06-based NDM values ranged from 40 to 70 months, with lower drought frequency mainly in the west and south. MaxSev remained low in most areas, indicating few extreme drought episodes. However, localized peaks in MaxInt, especially in the western zone, suggest that although droughts were shorter, some were notably intense.

In contrast, the period 2012–2023 saw a marked increase in drought severity and persistence. NDM values rose significantly, exceeding 80 months in the western region, indicating sustained moisture deficits. MaxSev increased sharply, especially in the northern and northeastern areas, where values surpassed 50, highlighting a shift toward more extreme droughts. MaxInt also intensified, with peak intensities now concentrated in the northeast, suggesting the emergence of severe and long-lasting drought episodes in these zones. Comparing the two periods shows a clear intensification of drought conditions over time. The northern and northeastern areas have become drought hotspots with the highest frequency, severity, and intensity. These trends point to growing vulnerability to climatic extremes, emphasizing the need for targeted, region-specific drought adaptation strategies, particularly in areas at greatest risk of persistent moisture deficits.

Trend detection and magnitude estimation

In this study, the non-parametric Mann–Kendall test and Sen's slope estimator were applied to SPEI03 and SPEI06 time series to detect and quantify monotonic trends in drought dynamics across the study area. Fig. 5 displays the spatial distribution of trend significance (p-values), trend direction (M-K statistic), and

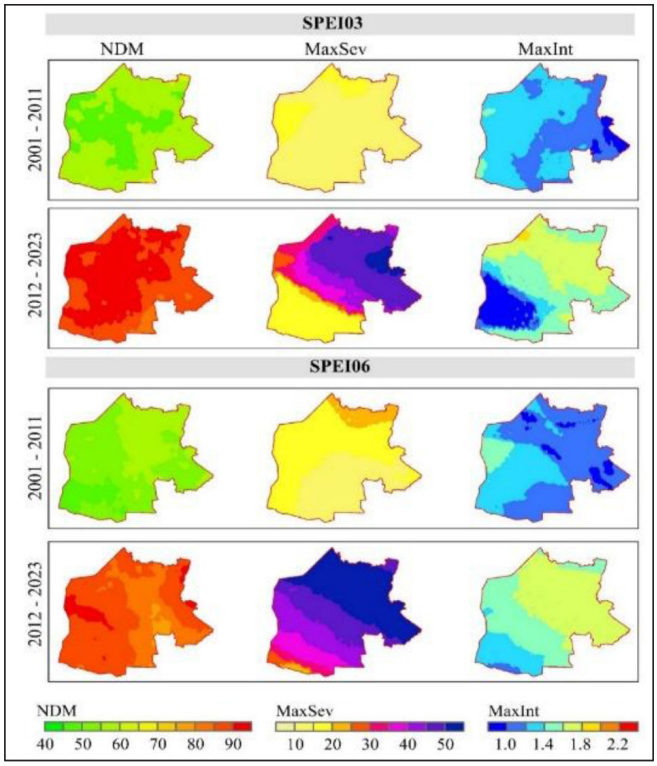

Fig. 4: Spatial distribution of drought metrics (NDM, MaxSev, MaxInt) for the SPEI03 and SPEI06 during two periods (2001–2011 & 2012–2023)

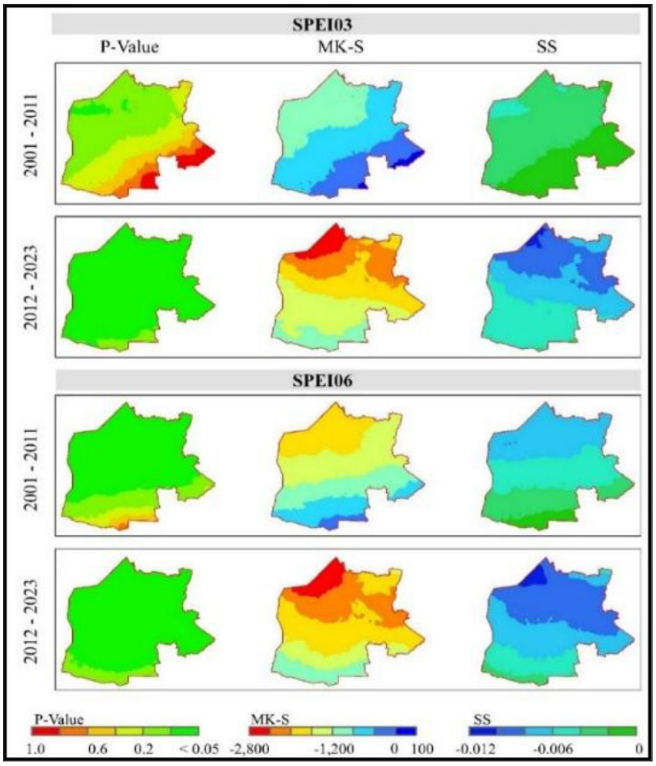

Fig. 5: Spatial distribution of Mann-Kendall trend significance (P-Value), trend direction (MK-S), and magnitude of change (Sen's Slope) for SPEI03 and SPEI06 during two periods (2001–2011 & 2012–2023)

trend magnitude (SS) for both indices. During 2001-2011, SPEI03 indicated predominantly negative trends, with more pronounced drying in the northern and northeastern regions. SPEI06 exhibited a more substantial negative trend, particularly in the northern areas, suggesting stronger medium-term drying, likely a result of cumulative precipitation deficits and increased evapotranspiration. In the 2012-2023 period, both indices showed a marked intensification of drought conditions. SPEI03 revealed broader and stronger negative trends, especially in the northern and northeastern zones, where Sen's Slope values indicated substantial reductions in moisture. SPEI06 demonstrated a widespread and consistent decline across the entire region, with trend magnitudes and significance surpassing those observed in the earlier period.

These findings highlight a clear acceleration in drought severity over time. The transition from localized to region-wide drying, coupled with the statistical significance of the trends, underscores a shift toward more persistent arid conditions. This intensification signals an urgent need for regionally tailored water resource management and climate adaptation strategies to mitigate the escalating impacts of prolonged drought in the study area.

CONCLUSION

This spatiotemporal analysis of drought characteristics using SPEI03 and SPEI06 reveals a clear and concerning trend of increasing drought severity and frequency, indicating a progressive shift toward greater aridity across the study area. Analysis using SPEI03 and SPEI06 indicates a marked intensification of drought conditions over the past two decades, with the years 1999, 2000, 2008, and 2021 identified as critical periods characterized by widespread and prolonged dry spells. A temporal comparison between the periods 2001–2011 and 2012–2023 demonstrates a transition toward more persistent and extreme drought events. At the station level, Tel-Afar exhibited the most prolonged and severe drought conditions, while the western and southern regions showed a notable increase in drought intensity. The spatial heterogeneity of drought impacts was further corroborated by the Mann-Kendall trend test and Sen's slope estimator. Collectively, these insights underscore the expansion of drought-affected areas and the ongoing shift toward more arid conditions, reinforcing the urgent need for adaptive water resource management and enhanced climate resilience strategies.

This study is limited by the small number of meteorological stations available in Nineveh, which constrains the spatial representation of observed data. Although bias-corrected TerraClimate data were used to overcome this limitation, evaluating other gridded datasets such as CHIRPS, ERA5-Land, or TAMSAT could further improve regional drought accuracy. Future work should also integrate machine learning approaches with multi-source remote sensing data to enhance drought prediction, mapping, and early warning in data-scarce regions like northern Iraq.

ACKNOWLEDGEMENT

The authors thank the School of Civil Engineering, Universiti Sains Malaysia (USM) for providing the necessary

facilities for the research work.

Funding: This research did not receive any financial support.

Conflict of interest: The authors report no conflicts of interest.

Data availability: The data supporting this study are available from the corresponding author upon reasonable request.

Authors contribution: **K. Qaraghuli**: Conceptualization, Methodology, Visualization; Writing-original draft; **M. F. Murshed**: Supervision, Methodology, Reviewing, and Editing; **M. A. M. Said**: Supervision, Reviewing, and Editing.

***Disclaimer**:* The contents, opinions, and views expressed in the research article published in the Journal of Agrometeorology are the views of the authors and do not necessarily reflect the views of the organizations they belong to.

Publisher's Note: The periodical remains neutral with regard to jurisdictional claims in published maps and institutional affiliations.

REFERENCES

Al-Yaari, A., Condom, T., Anthelme, F., Cauvy-Fraunié, S., Dangles, O., Junquas, C., Moret, P., & Rabatel, A. (2024). Warming-induced cryosphere changes predict drier Andean eco-regions. *Environmental Research Letters*, *19*(10). https://doi.org/10.1088/1748-9326/ad6ea6

Hashim, B. M., Alnaemi, A. N. A., Sultan, M. A., Alraheem, E. A., Abduljabbar, S. A., Halder, B., Shahid, S., & Yaseen, Z. M. (2025). Impact of climate change on land use and relationship with land surface temperature: representative case study in Iraq. *Acta Geophysica*. https://doi.org/10.1007/s11600-024-01514-0

Mokhtar, A., He, H., Alsafadi, K., Mohammed, S., Ayantobo, O. O., Elbeltagi, A., Abdelwahab, O. M. M., Zhao, H., Quan, Y., Abdo, H. G., Gyasi-Agyei, Y., & Li, Y. (2022). Assessment of the effects of spatiotemporal characteristics of drought on crop yields in southwest China. *International Journal of Climatology*, *42*(5), 3056-3075. https://doi.org/10.1002/joc.7407

Newman, A. J., Kalb, C., Chakraborty, T. C., Fitch, A., Darrow, L. A., Warren, J. L., Strickland, M. J., Holmes, H. A., Monaghan, A. J., & Chang, H. H. (2024). The High-resolution Urban Meteorology for Impacts Dataset (HUMID) daily for the Conterminous United States. *Scientific Data* , *11*(1), 1-16. https://doi.org/10.1038/s41597-024-04086-2

Prasad, A., Singh, R. K., K V Ramana Rao, & C. K. Saxena. (2025). Applicability of machine learning models for drought prediction using SPI in Kalahandi, Odisha. *Journal of Agrometeorology*, *27*(2), 216-220. https://doi.org/10.54386/jam.v27i2.2906

Qaraghuli, K., Murshed, M. F., M. Said, M. A., Mokhtar, A., & Rousta, I. (2024). Univariate and multivariate imputation methods evaluation for reconstructing climate time series data: A case study of Mosul station-Iraq. *Journal of Agrometeorology*, *26*(3), 318-323. https://doi.org/10.54386/jam.v26i3.2657

Rahman, G., Jung, M.-K., Kim, T.-W., & Kwon, H.-H. (2025). Drought impact, vulnerability, risk assessment, management and mitigation under climate change: A comprehensive review. *KSCE Journal of Civil Engineering*, *29*(1), 100120. https://doi.org/10.1016/j.kscej.2024.100120

Sa'adi, Z., Yusop, Z., Alias, N. E., Chow, M. F., Muhammad, M. K. I., Ramli, M. W. A., Iqbal, Z., Shiru, M. S., Rohmat, F. I. W., Mohamad, N. A., & Ahmad, M. F. (2023). Evaluating Imputation Methods for rainfall data under high variability in Johor River Basin, Malaysia. *Applied Computing and Geosciences*, *20*(July), 100145. https://doi.org/10.1016/j.acags.2023.100145

Terzi, T. B., & Önöz, B. (2025). Advanced drought analysis using a novel copula-based multivariate index: a case study of the Ceyhan River Basin. *Sustainable Water Resources Management*, *11*(1), 11. https://doi.org/10.1007/s40899-025-01189-5

Vicente-Serrano, S. M., Beguería, S., & López-Moreno, J. I. (2010). A multiscalar drought index sensitive to global warming: The Standardized Precipitation Evapotranspiration Index. *Journal of Climate*, 23(7), 1696–1718. https://doi.org/10.1175/2009JCLI2909.1